Applied Computer Science, vol. 13, no. 4, pp. 56–64
doi: 10.23743/acs-2017-29

Submitted: 2017-10-30
Revised: 2017-11-15
Accepted: 2017-12-06

Abaqus Finite Elements, Plane Stress, Orthotropic Material

Bartosz KAWECKI[*], *Jerzy PODGÓRSKI*[*]

NUMERICAL RESULTS QUALITY IN DEPENDENCE ON ABAQUS PLANE STRESS ELEMENTS TYPE IN BIG DISPLACEMENTS COMPRESSION TEST

Abstract

The paper presents a brief description of the Abaqus Simulia plane stress quadrilateral elements (CPS4R, CPS4I, CPS4, CPS8R, CPS8). Comparison of the results quality obtained using each of them was done. There was considered two dimensional big displacements compression test for a highly orthotropic material. Simulations were performed for the compression in two perpendicular directions.

1. INTRODUCTION

Abaqus Simulia software makes many finite elements available to its users. The basic problem is the criterion of choosing an appropriate element to the specific investigation.

The paper presents the description of five plane stress quadrilateral elements available in Abaqus. Brief outline of nodes, degrees of freedom and the Lagrange polynomial shape functions was done (Zienkiewicz 2000, Bathe 2014, Liu 2014). The paper provides a comparison of the results obtained for a highly orthotropic material using each of elements in a big displacements compression test. Constitutive law for the material was defined basing on (Jones 1999, Lekhnitskii 1981). The general aim of the numerical experiment was the need of determination element's suitability for usage in the analyses, where considerable distortion of the elements is anticipated. The problem of oversize distortion was raised in several papers (Macneal 1985, Barlow 1989, Lee 1993).

[*] Lublin University of Technology, Faculty of Civil Engineering and Architecture, Department of Structural Mechanics, Nadbystrzycka 40, 20-618 Lublin, Poland, b.kawecki@pollub.pl, j.podgorski@pollub.pl

As a report from numerical analyses there was specified σ_{11} and σ_{22} stress distribution in dependence on element type, direction of compressing and applied mesh. Modelling and mesh study was based on the scientific papers (Turcke 1974, Cecil 1994). Additionally, there were prepared diagrams of P-δ relation to notice any discontinuities or disturbances in the model. Basing on the numerical results there were made general conclusions and recommendations for using the Abaqus plane stress quadrilateral elements with highly orthotropic materials.

2. ELEMENTS DESCRIPTION

The simplest elements are 4-node bilinear plane stress quadrilateral elements, which are presented in Fig.1.

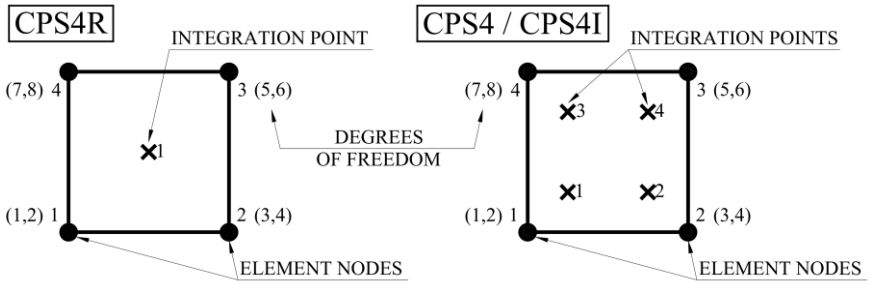

Fig. 1. Linear geometric order (first order) plane stress elements (author's study basing on Abaqus User's Manual)

The difference between CPS4 and CPS4I is an occurrance of the additional internal degrees of freedom preventing the element from overly stiff behavior in bending, called shear locking. The phenomenon is more precisely described in (Cook 2002) and Abaqus User's Manual.

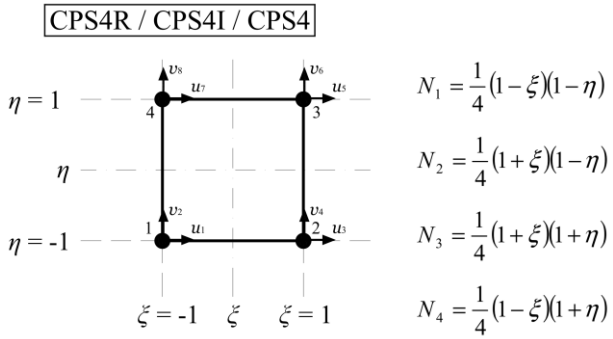

Fig. 2. 4-node element shape functions based on Lagrange polynomials

General functions describing work of the finite elements are the shape functions (Zienkiewicz 2000, Bathe 2014, Liu 2014). In most cases they are based on Lagrange polynomials. Defining coordinate system using η and ξ axes, shape functions may be written as it was shown in Fig.2. Denotations u and v describe nodal translation degrees of freedom. More complex elements are 8-node biquadratic plane stress quadrilateral elements, which are presented in Fig.3.

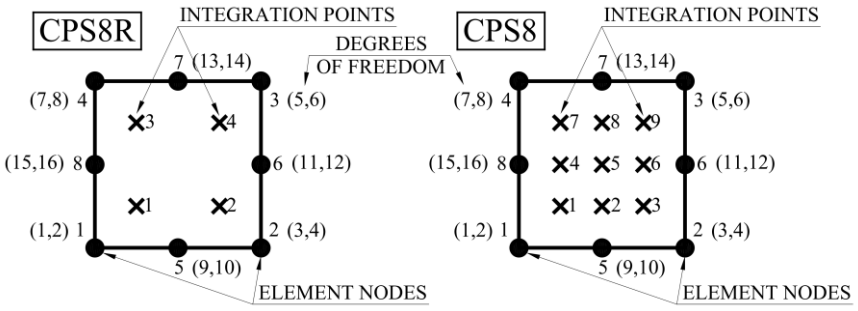

Fig. 3. Quadratic geometric order (second order) plane stress elements (author's study basing on Abaqus User's Manual)

Defining coordinate system as before, using η and ξ axes, shape functions may be written as it was shown in Fig.4. Denotations u and v describe nodal translation degrees of freedom.

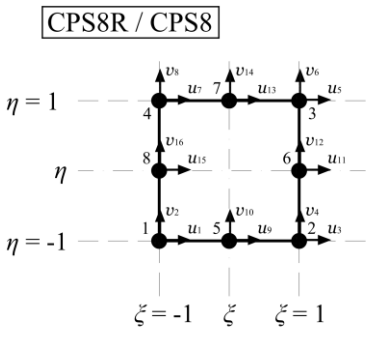

$$N_1 = \frac{1}{4}(1-\xi)(1-\eta)(-\xi-\eta-1) \qquad N_5 = \frac{1}{2}(1-\xi^2)(1-\eta)$$

$$N_2 = \frac{1}{4}(1+\xi)(1-\eta)(\xi-\eta-1) \qquad N_6 = \frac{1}{2}(1+\xi)(1-\eta^2)$$

$$N_3 = \frac{1}{4}(1+\xi)(1+\eta)(\xi+\eta-1) \qquad N_7 = \frac{1}{2}(1-\xi^2)(1+\eta)$$

$$N_4 = \frac{1}{4}(1-\xi)(1+\eta)(-\xi+\eta-1) \qquad N_8 = \frac{1}{2}(1-\xi)(1-\eta^2)$$

Fig. 4. 8-node element shape functions based on Lagrange polynomials

In both 4-node and 8-node elements the equation given below is met:

$$\sum_{i=1}^{n} N_i = 1 \tag{1}$$

Displacement field is described by formula:

$$u = \sum_{i=1}^{n} N_i u_i \qquad v = \sum_{i=1}^{n} N_i v_i \tag{2}$$

In both elements types there are considered reduced and full integration modes. Reduced integration provides lower computational cost in the numerical analysis, but on the other hand may lead to the lower quality of the results. These aspects will be discussed in the next paragraph.

3. COMPRESSION TEST FEM MODEL

There were prepared two numerical models with different local coordinate systems orientations. For highly orthotropic materials, orientation of the specimen is crucial for obtained stresses and strains values.

Fig. 5. a) presents set of compression in a longitudinal direction, and Fig. 5. b) set of compression in a transversal direction. Predicted results of the stresses distribution should be completely different from each other.

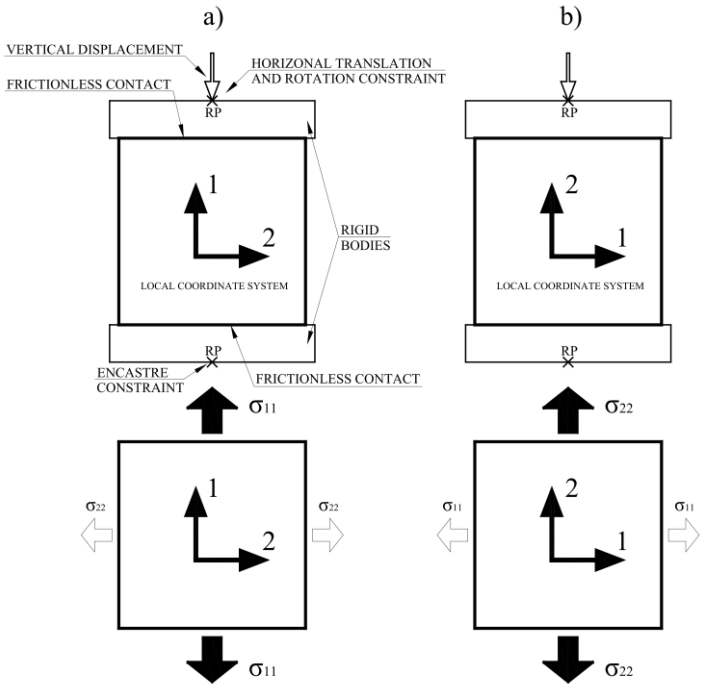

Fig. 5. Compression test with different local coordinate systems orientation: a) longitudinal compression, b) transversal compression

Compressing steel parts were modeled as rigid bodies to prevent them from deformations. Lower support was fixed in the reference point, upper steel plate was constrained in the horizontal direction and in the plane rotation. There was added constant vertical displacement of the upper steel plate and frictional contact between the specimen and steel plates.

There were two mesh sizes taken into account: 16 elements and 64 elements, which is presented in Fig.6.

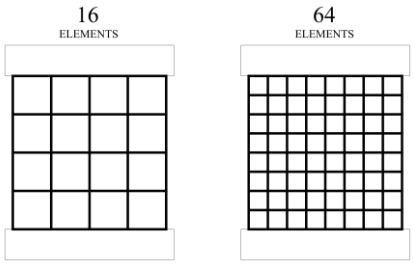

Fig. 6. Number of finite elements used in the numerical simulation

For both directions of compression there was added the same vertical displacement δ = 5 mm.

4. NUMERICAL RESULTS

Numerical results contain comparison of the elements behaviour under big displacement compression and description of σ_{11} and σ_{22} stresses distribution in the specimen. Expected values σ_{11} stresses were much higher than σ_{22} because of a great difference in the elastic modules depending on the direction. For better understanding work of the whole specimen there were made diagrams with P-δ relation. Results for mesh with 16 elements are shown in Fig.7–11.

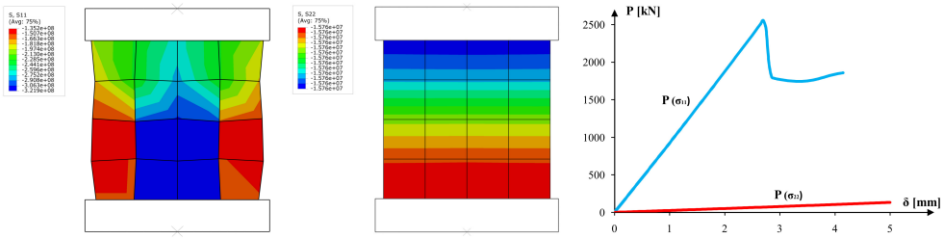

Fig. 7. CPS4R elements displacements, σ_{11}, σ_{22} stresses distribution and P-δ relation

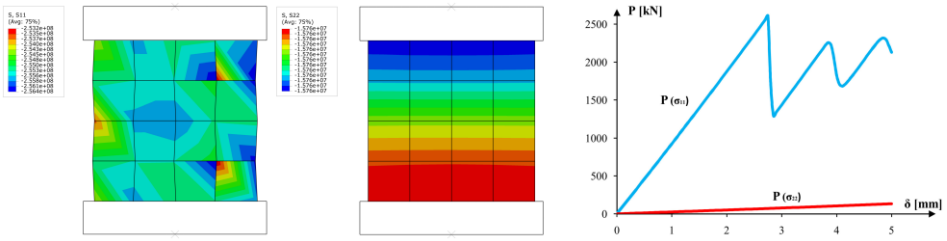

Fig. 8. CPS4I elements displacements, σ_{11}, σ_{22} stresses distribution and *P-δ* relation

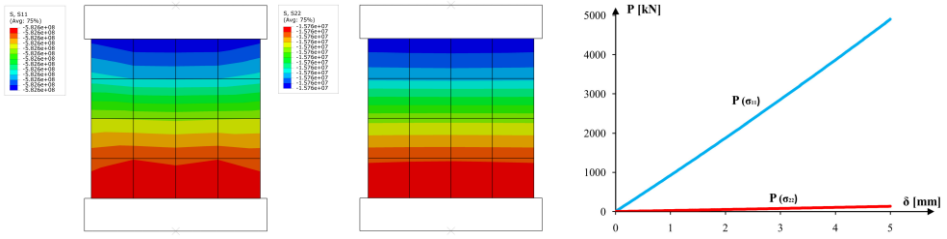

Fig. 9. CPS4 elements displacements, σ_{11}, σ_{22} stresses distribution and *P-δ* relation

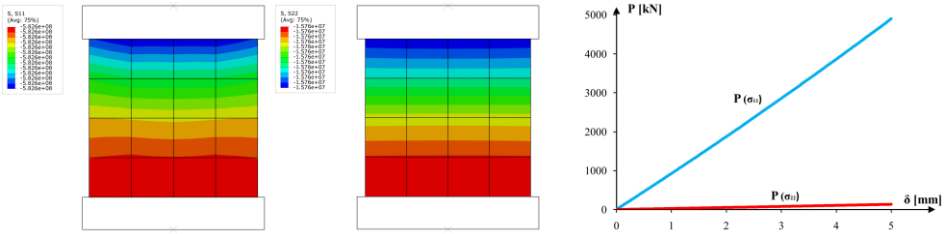

Fig. 10. CPS8R elements displacements, σ_{11}, σ_{22} stresses distribution and *P-δ* relation

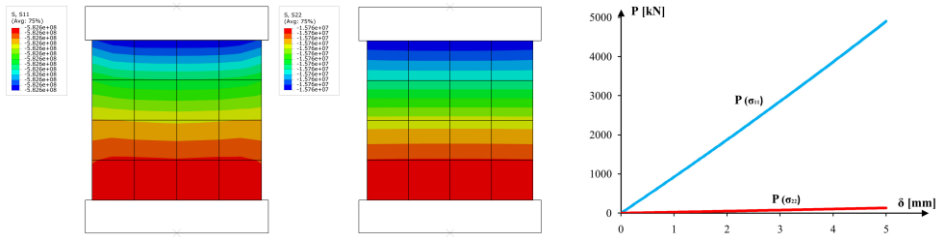

Fig. 11. CPS8 elements displacements, σ_{11}, σ_{22} stresses distribution and *P-δ* relation

CPS8 presented the most precise results. Comparing other elements to the CPS8 it was visible that CPS8R and CPS4 gave accurate results while CPS4I and CPS4R gave inaccurate results in σ_{11} direction, due to the excessive elements distortion.

Additionally, for CPS4R element, analysis convergence ends in about 80% of the analysis progress and the shape of the elements is unphysical. *P-δ* relation diagrams clearly shows the disturbances in the whole model caused by CPS4R and CPS4I elements, while for CPS4, CPS8R and CPS8 relation is smooth.

General principal to get the proper results from the numerical model was considering lower and higher mesh density. Only then an interpretation of the results might be correct. Because of that there was prepared the second mesh with 64 finite elements in the specimen. This approach allowed to find out how mesh density influence the solution. Results of the investigation are presented in Fig.12–16.

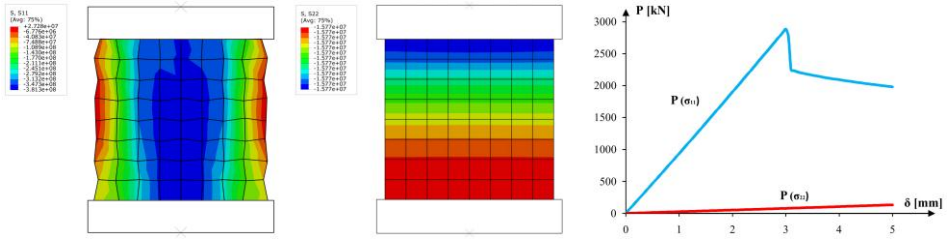

Fig. 12. CPS4R elements displacements, σ_{11}, σ_{22} stresses distribution and *P-δ* relation

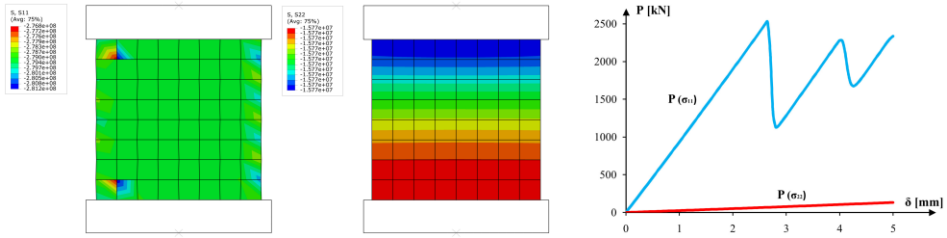

Fig. 13. CPS4I elements displacements, σ_{11}, σ_{22} stresses distribution and *P-δ* relation

The same as in case of 16 elements mesh, there were visible inaccurate stress results for CPS4R and CPS4I. It seemed that mesh density had a low influence on the elements work. There was a visible progress in proper stress distribution range in case of CPS4R elements, however after reaching some stress limit, these elements behaviour was still unphysical.

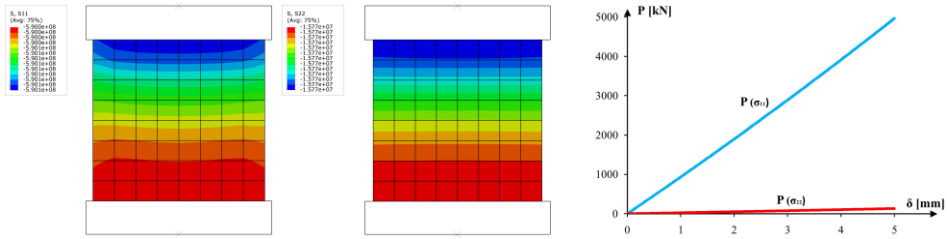

Fig. 14. CPS4 elements displacements, σ_{11}, σ_{22} stresses distribution and *P-δ* relation

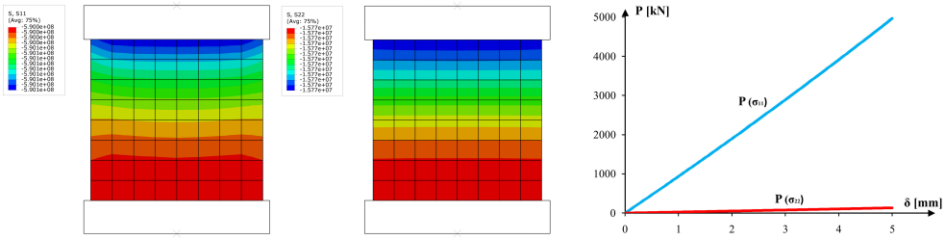

Fig. 15. CPS8R elements displacements, σ_{11}, σ_{22} stresses distribution and *P-δ* relation

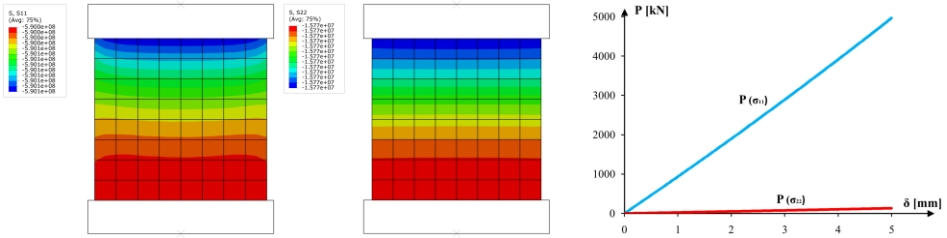

Fig. 16. CPS8 elements displacements, σ_{11}, σ_{22} stresses distribution and *P-δ* relation

5. CONCLUSIONS

Basing on the performed numerical analyses there were made several conclusions about using Abaqus plane stress quadrilateral elements.

CPS4R and CPS4I elements were recommended only to use with small displacements and linear problems. Nonlinearity would probably cause similar inadequate effects as an orthotropic material as presented in the paper. In case of these finite elements, making mesh more dense may have no influence on getting better numerical results.

CPS4 elements gave the same good results in the compression as CPS8R and CPS8 elements. However it was worth to remember that shear locking occurs in CPS4 elements.

The best solution for almost all of the plane stress problems are second order quadrilateral elements CPS8R and CPS8, which give proper results in compression, big displacements, works well with highly orthotropic materials and with bending.

The author's study provides precise information about how the Abaqus plane stress elements work under compression. It is a very important case for a further research. There are planned several numerical modelling validations in delamination and damage processes in highly orthotropic materials. It is possible only when accurate results are provided by the finite elements.

REFERENCES

Abaqus/CAE V6.14 User's Manual.

Armstrong, C. G. (1994), Modelling requirements for finite-element analysis. In *Computer-Aided Design*, Vol. 26, 573–578, https://doi.org/10.1016/0010-4485(94)90088-4.

Barlow, J. (1989), More on optimal stress points – reduced integration, element distortions and error estimation. *International Journal of Numerical Methods in Engineering*, Vol. 28, 1487–1504, doi:10.1002/nme.1620280703.

Bathe, K. J. (2014). Finite Element Procedures. Second Edition, 341–389.

Cook R. D., Malkus, D.S., Plesha M. E., Witt R.J.(2002), Concepts and Applications of FEA, 4th ed., John Wiley&Sons, Inc., 98–102.

Jones, R. M. (1999), Mechanics of Composite Materials. Second Edition, 55–73.

Lekhnitskii S.G. (1981), Theory of Elasticity of an Anisotropic Elastic Body, Mir Publishers.

Lee, N. S., & Bathe, K. J. (1993), Effects of element distortions on the performance of isoparametric elements. *International Journal of Numerical Methods in Engineering*, Vol. 36, 3553–3576, doi:10.1002/nme.1620362009.

Liu, G. R. & Quek, S. S. (2014), The Finite Element Method. A Practical Course. Second Edition, 161–211.

Macneal, R. H., & Harder, R. L. (1985), A proposed standard set of problems to test finite element accuracy. In *Finite Elements in Analysis and Design*, Vol. 1, 3–20, https://doi.org/10.1016/0168-874X(85)90003-4.

Turcke, D. J., & McNeice, G. M. (1974), Guidelines for selecting finite element grids based on an optimization study. In Computers & Structures, Vol. 4, 499–519, https://doi.org/10.1016/0045-7949(74)90003-0.

Zienkiewicz, O. C., & Taylor, R. L. (2000). The Finite Element Method. Fifth Edition. Volume 1: The Basis, 164–198.